View Article Online
View Journal

Green Chemistry

Cutting-edge research for a greener sustainable future

Accepted Manuscript

This article can be cited before page numbers have been issued, to do this please use: M. Y. Suleman, H. L. Judah, P. Bexis, P. Fennell, J. P. Hallett and A. Brandt-Talbot, *Green Chem.*, 2025, DOI: 10.1039/D5GC02409A.

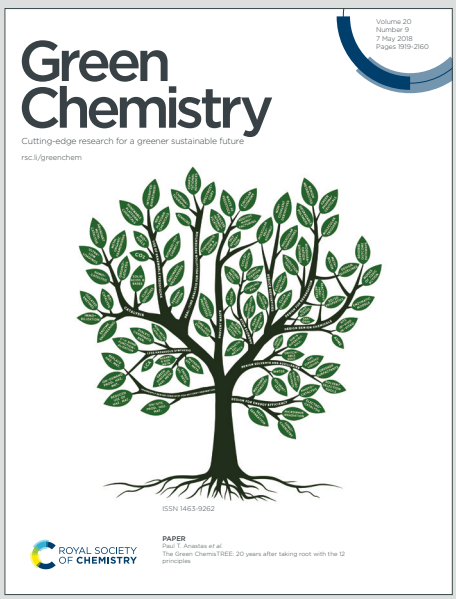

ROYAL SOCIETY OF CHEMISTRY

rsc.li/greenchem

View Article Online
DOI: 10.1039/D5GC02409A

Green Foundation Box

1. **How does your work advance the field of green chemistry?**
   This work advances green chemistry by identifying water-containing ionic liquids, especially the low-cost protic ionic liquids such as 1-methylimidazolium acetate [C_1Him][OAc], as effective media for PET depolymerisation. Using the solvent mixture offers milder reaction conditions compared to conventional methods. The approach supports circular economy goals by enabling chemical recycling of plastic waste.

2. **Please can you describe your specific green chemistry achievement, either quantitatively or qualitatively.**
   Employing [C_1Him][OAc] with 15 wt% water, the study achieved 98.5% PET conversion and 82.4% crude TPA yield with 77.8% purity using moderate hydrolysis conditions (180 °C, 3 h). The IL is easy to prepare and low-cost (~$2/kg), with is >10 times lower than the cost of the analogous aprotic ionic liquid solvent. The study also introduced chromatographic purity analysis, improving the accuracy of performance evaluation over purely gravimetric methods.

3. **How could your work be made greener and be elevated by further research?** Future work should develop monomer recovery methods that avoid acid addition to avoid waste during monomer isolation and enable IL reuse and demonstrate higher. Research into IL recyclability, process intensification (higher loading), and application to mixed and degraded plastic waste will enhance the environmental and practical impact of this method.

View Article Online
DOI: 10.1039/D5GC02409A

The acetate anion promotes hydrolysis of poly(ethylene terephthalate) in aprotic and protic ionic liquid water mixtures

Maariyah Y. Suleman,[a‡] Harriet L. Judah,[a‡] Panagiotis Bexis,[a] Paul Fennell,[b] Jason P. Hallett[b] and Agnieszka Brandt-Talbot[a]*

[a] Department of Chemistry, Imperial College London, London, W12 0BZ, UK

[b] Department of Chemical Engineering, Imperial College London, London, SW7 2AZ, UK

‡ These authors contributed equally to this work

*Corresponding author: agi@imperial.ac.uk

Abstract

A circular plastic economy reduces raw material consumption and discourages pollution. Chemical recycling upgrades the quality of recyclate and is a complementary approach to thermomechanical recycling of plastic waste. This study investigated the use of aprotic and protic ionic liquids (ILs) as solvents for chemical recycling by hydrolysis of the most common polyester plastic, poly(ethylene terephthalate) (PET). Combinations of three types of cations (aprotic 1-alkyl-3-methylimidazolium, protic 1-methylimidazolium and protic 1,5-biazocyclo-[4.3.0]non-5-enium) combined with a range of anions (acetate, chloride, methanesulfonate, hydrogen sulfate, methyl sulfate, trifluoromethanesulfonate and chlorozincate) were used to hydrolyse PET in the presence of 15 wt% water as the co-solvent and reagent. PET conversion at the screening conditions (180 °C, 3 h, 5% PET loading) varied between 1 – 100%, with ILs containing the acetate anion enabling >97% PET conversion irrespective of the cation. Acidification with aqueous HCl recovered crude crystallised terephthalic acid (TPA). Significant crude yields (46 – 93%) were only observed for the acetate ILs. The purity of the crude TPA was 34 – 98%, with 1-ethy-3-methylimidazolium acetate, [C_2C_1im][OAc], and 1-methylimidazolium acetate, [C_1Him][OAc], yielding more and purer TPA than 1,5-biazocyclo-[4.3.0]non-5-enium acetate, [DBNH][OAc]. TPA solubility at 5% solid loading was measured and correlated with increasing pK_a and hydrogen bond acceptor strength of the IL anion. PET conversion and TPA yield generally correlated well with TPA solubility, suggesting that the depolymerisation mechanism in the acetate ILs is base catalysed. The screening identifies aqueous mixtures of the (pseudo) protic IL [C_1Him][OAc] as promising catalytic solvents for the chemical recycling of PET at an industrially feasible temperature, due to high isolated TPA yields and good purity at low ($1.74-2.15/kg) solvent cost. However, an effective separation approach for the monomers TPA and ethylene glycol from the solvent remains to be developed.

Keywords: Chemical reycling, Terephthalic acid, Depolymerisation, Plastic, PET, Solubility

View Article Online
DOI: 10.1039/D5GC02409A

Introduction

PET is a commodity plastic that is widely used in applications such as packaging, construction, textiles and electronics,[1, 2] accounting for 6.2% of global plastic production.[3, 4] The European PET bottle recycling rate was 50% in 2022, which was achieved through thermomechanical recycling, consisting of shredding waste PET to produce flakes that can be melted and re-extruded into recycled plastic pellets. Thermomechanical recycling is a well-developed technology, however, the recycled plastic typically has degraded material properties. For example, it is coloured or has reduced mechanical strength, caused by lower molecular weight and contamination with other polymers and materials.[5, 6] As a result, mechanically recycled PET from bottles and food packaging is often used in applications with less stringent specifications for mechanical strength and transparency, such as polyester textiles, while polyester textiles remain unrecycled.[7] To encourage the use of recycled PET in food packaging and make coloured polyester textiles recyclable, methods to purify and upgrade PET-containing waste are required.[8]

Chemical plastic recycling encompasses a variety of methods that employ heat or chemical agents to separates additives from the polymer or to break the chemical bonds in polymer, which recovers chemical feedstocks or purified oligomers or monomers.[9] Biological plastic recycling employs microorganisms or enzymes to break chemical bonds in polymers to facilitate recycling at the oligomer or monomer level.[10] PET is a condensation polymer and can be chemically recycled by cleaving the ester bonds, typically using a solvent containing nucleophiles such as water, glycols, alcohols, and amines, yielding a range of depolymerisation products (Figure 1). [6, 9, 11, 12, 13] Challenges for chemical recycling *via* depolymerisation include avoiding the generation of by-products and chemical waste, and minimising the energy requirement for depolymerisation and monomer recovery.[14] PET is sparingly soluble in most solvents due to its high molar weight and crystallinity.[15] As a result, PET is typically depolymerised at the solid-liquid interface, including for approaches that employ ILs.[16-18]

Glycolysis of PET with ethylene glycol (EG) as the monomer, solvent and nucleophile is the most investigated approach, generating solubilised bis(2-hydroxyethyl) terephthalate (BHET) and EG. However, glycolysis faces challenges during purification, such as slow crystallisation of crude BHET at low temperatures, which requires cooling to 0 – 10 °C for up to 24 hours.[19, 20] Recently, depolymerisation of PET in anhydrous acetic acid has been reported as an approach called acetolysis, yielding TPA and acetylated EG after evaporating the solvent.[13] While acetolysis results in rapid crystallisation of TPA, it requires anhydrous conditions and high temperatures (>280 °C).[13]

View Article Online
DOI: 10.1039/D5GC02409A

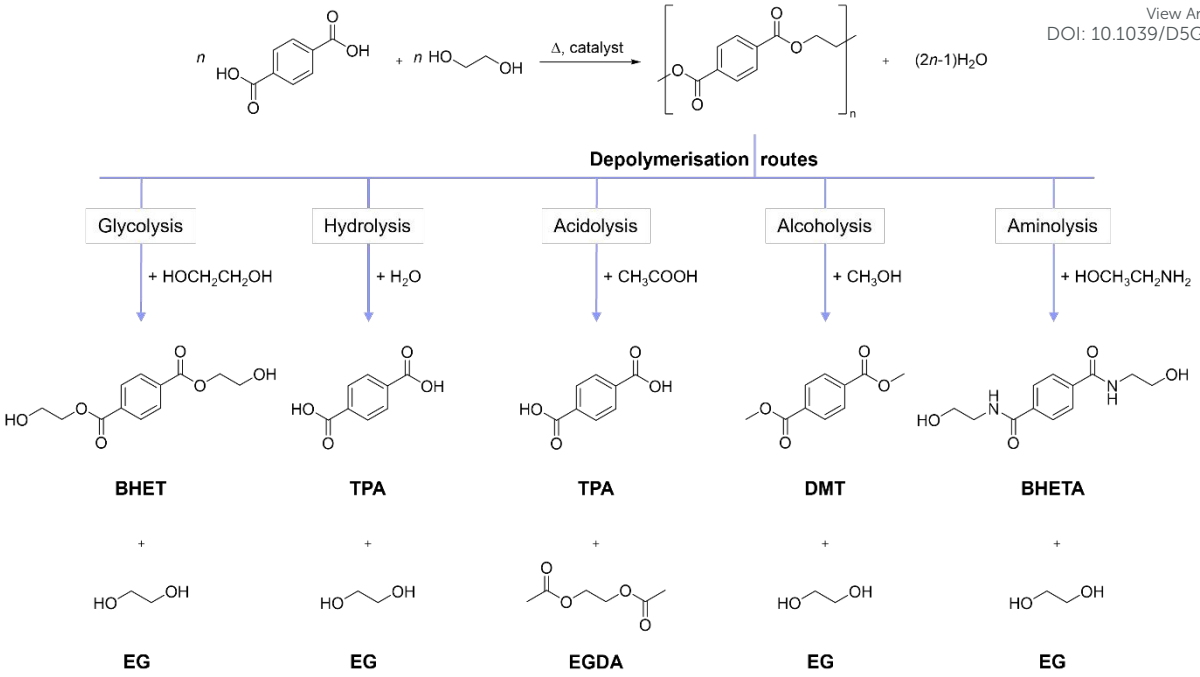

Figure 1: Industrial production of PET and depolymerisation routes using various nucleophiles which produce terephthalic acid, bis(2-hydroxyethyl) terephthalate, dimethyl terephthalate, bis(2-hydroxyethyl) terephthalamide, ethylene glycol (EG) or ethylene glycol diacetate (EGDA).

The depolymerisation of PET using water as the nucleophile (hydrolysis) is attractive, as it is a direct reversal of the industrial PET production method (Figure 1), however, TPA is not soluble in neutral or acidic water. Without a suitable catalyst, high temperatures and pressures or long reaction times are required to achieve depolymerisation.[21] Catalysts for PET hydrolysis can be inorganic and organic hydroxides, Lewis acids, ILs and deep eutectic solvents. PET hydrolysis has been carried out using aqueous solutions of sodium hydroxide at 50 – 80°C, yielding crystallised TPA and EG.[22] The TPA could only be isolated after reducing the pH by adding HCl or H_2SO_4 to protonate the deprotonated terephthalate, which creates salt waste (NaCl or Na_2SO_4). PET was hydrolysed at 80 – 120 °C within 1 h using mixtures of metal salt hydrates and organic acids, reporting PET conversion and an isolated crude TPA yield up to 100% and 96.4%, respectively. TPA precipitation occurred without the need to adjust the pH, instead, with water used as an anti-solvent.[23] Enzymes are effective at hydrolysing PET at low temperatures (55 °C), but reactions times are long (4 days) and addition of acid is required to precipitate the TPA.[24]

ILs have been used as catalysts or catalytic solvents for PET depolymerisation, with IL-assisted glycolysis the most commonly reported approach. The IL is used as a catalyst (approx. 5 wt% loading relative to EG) to accelerate the reaction or to replace the inorganic Lewis acidic catalyst, $Zn(OAc)_2$.[16, 25-27] A number of protic ILs have been reported for PET glycolysis, examples include triazabicylodecanium methanesulfonate, [TBD][CH_3SO_3],[28] 1,5-diazabicyclo[4.3.0]non-5-enium 4-methylphenoxide, [DBNH][4-CH_3PhO],[27] 1,8-

View Article Online
DOI: 10.1039/D5GC02409A

diazabicyclo[5.4.0]undec-7-enium imidazolate, [HDBU][Im],[29] 1,5,7-triazabicyclo[4.4.0]dec-5-enium acetate, [TBD][OAc],[30] and 2-hydroxyethyl ammonium acetate, [2-HEAA][OAc],[31] with complete PET conversion and BHET yields of at least 85%.

IL-assisted hydrolysis of PET has been less commonly reported. Hydrolysis of PET (polyester) fibre employing mixtures of 1-butyl-3-methylimidazolium hydrogen sulfate, $[C_4C_1im][HSO_4]$, or 1-methylimidazolium hydrogen sulfate, $[C_1Him][HSO_4]$, with 40 - 60 wt% water was demonstrated,[32] with PET conversion up to 80% at 185 – 195 °C after 2.5 – 3.5 h, while TPA yield and purity were not quantified. 1-Butyl-3-methylimidazolium chloride, $[C_4C_1im]Cl$, accelerated PET fabric hydrolysis as a 5% additive in aqueous and methanolic solutions of sodium hydroxide.[33] Choline lysinate, [Ch][Lys], enabled PET hydrolysis after 2 h at 180 °C, achieving 55% conversion and 56% un-isolated TPA yield.[34] Hydrolysis of PET in aqueous choline phosphate, $[Ch]_3[PO_4]$, was employed at 120 °C, yielding crude crystallised TPA after 3 h upon acidification, with the TPA yield not reported.[35] Liu *et al*. used a mixture of $[C_4C_1im]Cl$, and 1-methyl-3-(3-sulfopropyl)-imidazolium hydrogen sulfate, $[HSO_3\text{-pmim}][HSO_4]$, and 40 wt% water to hydrolyse PET at 170 °C for 4.5 h, reporting 89% crude isolated TPA yield after adding acid.[36] A 94% isolated TPA yield was reported for 1-(3-propylsulfonic)-3-methylimidazolium chloride, $[HSO_3\text{-pmim}]Cl$, mixed with 75 wt% water at 210 °C after 24 h, also employing acidification to isolate the TPA.[37] PET hydrolysis was reported in the presence of "switchable ILs" generated from a range of amines, CO_2 and water in a pressure reactor, with a reaction temperature of 150 °C and reaction time of 6 – 24 h achieving up to ≥99% TPA yield upon acidification.[38] Only small groups (2-6) of ILs of aprotic and protic ILs have been compared for PET hydrolysis.

The product purity is often not considered in studies that report isolated TPA yields, while methods such as differential scanning calorimetry, thermogravimetric analysis, X-ray diffraction, mass spectrometry, and spectroscopic techniques can only qualitatively assess product purity.[16, 27] Acid-base titration was used to assess purity quantiatively,[13] however, it is not able to distinguish TPA from acetic acid, 2-hydroxyethyl terephthalic acid (HETA), and other carboxylic acid impurities such as *p*-toluic acid and 4-carboxybenzaldehyde. NMR spectroscopy can provide quantitative insight, chromatographic separation is superior in precision and should be used for quantitative assessment of product purity.

This study systematically investigated the influence of the IL structures (anion and cation) on PET conversion and TPA yield following PET hydrolysis, with over 20 IL compositions used and with a focus on easy-to-synthesise PILs, which are synthesised through a proton transfer from a Brønsted acid to an amine. The study also demonstrates that spectroscopic

View Article Online
DOI: 10.1039/D5GC02409A

and chromatographic analyses are important to correctly report TPA yield and monitor product purity.

Experimental

Materials

Reagents were used as received unless specified otherwise. PET beverage bottles were washed with deionised water and dried before cutting to 0.5 mm size particles (SM 2000, Retsch) followed by sieving through a 0.5 mm mesh. 1-Ethyl-3-methylimidazolium acetate, $[C_2C_1im][OAc]$, (>95%, 0.48% H_2O) and 1-butyl-3-methylimidazolium chloride, $[C_4C_1im]Cl$, (>98%, ≤1.0% H_2O) were purchased from IoLiTec Technologies (Germany). 1-Ethyl-3-methylimidazolium hydrogen sulfate, $[C_2C_1im][HSO_4]$, (95%, 0.14% H_2O), 1-butyl-3-methylimidazolium methyl sulfate, $[C_4C_1im][CH_3SO_4]$, (95%), DMSO-d_6 (99.96% atom% D), terephthalic acid (99%), 1-methylimidazole (99%), acetic acid (glacial, 99%), 1,3,5-trimethoxybenzene (≥99%) and HPLC-grade DMSO (≥99.7%) were purchased from Merck. Ethylene glycol (99.5%) was purchased from Acros Organics. 1,5-Diazabicyclo[4.3.0]non-5-ene (98%), trifluoromethanesulfonic acid (≥99%) and methanesulfonic acid (≥98%) were purchased from Fluorochem. Sulfuric acid (5 M) and hydrochloric acid (≥37%) were purchased from Honeywell-Fluka. Zinc chloride ($ZnCl_2$, ≥98%) was purchased from Alfa-Aesar. Sodium hydroxide (NaOH pellets, 98.5-100%) was purchased from AnalaR Normapur.

NMR spectroscopy

NMR spectra were recorded on a Bruker 400 MHz spectrometer at room temperature and processed using Mestre Nova software version 12 (Mestrelab Research, S.L., Santiago de Compostela, Spain). Chemical shifts (δ) are reported in parts per million (ppm). All NMR spectra were recorded in DMSO-d_6.

Synthesis of protic ionic liquids

Equimolar amounts of acid and amine (unless otherwise specified) were charged into a round-bottom flask with stir bar. The acid was added *via* dropwise addition through a dropping funnel. An ice bath was used to maintain the temperature below 5 °C. The mixture was stirred overnight at room temperature to ensure complete mixing. Deionised water was added as needed to produce ILs containing 15 wt% H_2O. $[C_4C_1im]Cl$, $[C_4C_1im][MeSO_4]$, [DBNH][OAc],

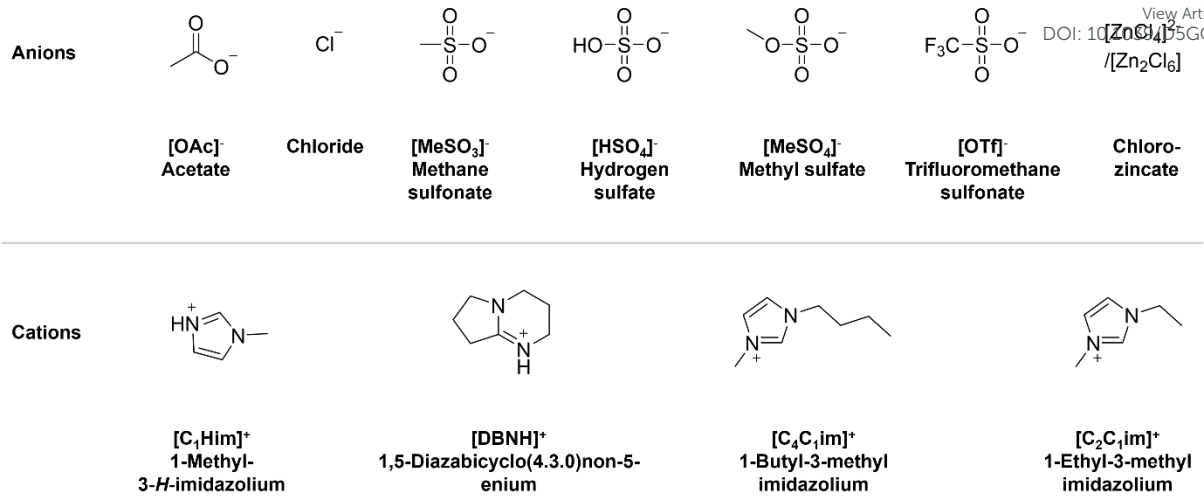

Figure 2: Structures of anions and cations used to construct protic and aprotic ILs in this work.

[DBNH][OAc] (1:2), [DBNH][OAc] (2:1), [DBNH][$MeSO_3$], [C_1Him][OTf] and [C_1Him][$MeSO_3$] were solid at room temperature, so were manually ground into powder and dried under vacuum before water was added. The water content of all synthesised ILs was adjusted to 15 wt%. If above this value, the water content was reduced using a rotary evaporator and measured using a volumetric Karl-Fischer titrator (Mettler Toledo titrator, Easyplus Easy KFV). All ILs used in this work are shown in Figure 2 and Table S1. Synthesised ILs were characterised with NMR spectroscopy and their detailed syntheses are described in the ESI (Figure S1 – S12).

PET hydrolysis

0.1 g PET powder and 2.0 g IL-water solution (15 ± 0.5 wt% water) were added to a 15 mL pressure tube (Aceglass) and sealed with a Teflon cap and O-ring (silicon or FETFE), forming a suspension with 5% PET loading according to Eq.1, in which m_{PET}, m_{IL} and m_{water} is the mass of each component:

$$PET\ loading(\%) = \frac{m_{PET}}{m_{IL} + m_{water}} \times 100 \qquad \text{(Eq.1)}$$

Samples were placed in a preheated oven (Binder ED 23, Binder GmbH) at the selected temperature (usually 180°C) for a selected length of time. After hydrolysis, the pressure tube was cooled to room temperature for at least 30 min. If a solid residue was present, 2 M sodium hydroxide was added until pH 10 – 11 was reached to dissolve TPA, using pH strips for monitoring. The remaining residue was assumed to be PET and separated via vacuum filtration using a Buchner funnel and Whatman™ 542 hardened ashless filter paper. The solid residue was washed with deionised water, dried in a vacuum oven at 60 °C for 24 h and the weight recorded. The weight was used to calculate PET conversion following Eq.2:

View Article Online
DOI: 10.1039/D5GC02409A

$$Conversion_{PET}(\%) = \frac{m_{PET_0} - m_{PET_1}}{m_{PET_0}} \times 100 \qquad \text{(Eq.2)}$$

Where m_{PET_1} is the weight of the residue (if present) and m_{PET_0} is the initial weight of the PET powder prior to hydrolysis.

To recover crude TPA, the filtrate was acidified with 37% aqueous HCl until pH 2 – 3 was reached (monitored using pH strips) and the solution became cloudy. The suspension was refrigerated (4 °C) for 24 h to complete precipitation, followed by vacuum filtration and washing with deionised water. The precipitate was dried in a vacuum oven for 24 h at 60 °C on the filter paper before recording the weight of isolated TPA. The crude TPA yield was calculated following Eq. 3:

$$Yield_{TPA\ crude}(wt\%) = \frac{m_{TPA}/M_{TPA}}{m_{PET,\,0}/M_{PET}} \times 100 \qquad \text{(Eq. 3)}$$

Where m_{TPA} is the weight of TPA product isolated after acidification, $m_{PET,\,0}$ is the initial weight of PET added to the IL-water mixture. M_{TPA} and M_{PET} are the molar weights of TPA (166 g/mol) and the PET repeating unit (192 g/mol), respectively.

Determination of TPA purity in crude product

The content of TPA in the crystallised product was determined using high performance liquid chromatography (HPLC) using an 1260 Infinity II Hybrid SFC/UHPLC (Agilent Technologies). The HPLC was equipped with an auto-sampler, C-18 column (Raptor C18, 50 × 2.1 mm, 2.7 µm) and a UV-Vis diode array detector, with 254 nm used for detection. A gradient of acetonitrile and 0.1% formic acid (aq) was used as the mobile phase. HPLC samples were prepared in HPLC-grade DMSO using 5.07 mM 1,3,5-trimethoxybenzene (TMB) as the internal standard. Calibration curves were prepared using purchased commercial TPA (99% purity). Isolated crude TPA (4 – 6 mg) was dissolved in a solution of dimethyl sulfoxide containing 5.07 mM TMB. The solution was filtered through a PTFE microfilter with 0.2 µm pore size to remove undissolved impurities and dust particles prior to analysis. A calibration curve for TPA was prepared ranging from 0.2 mM to 7.5 mM, and the calculated mass of TPA in the sample, $m_{TPA,calc}$, was determined via external calibration. TPA purity was calculated according to Eq. 4:

$$TPA\ mass\ purity\ (wt\%) = \frac{m_{TPA,calc}}{m_{TPA,sample}} \times 100 \qquad \text{(Eq. 4)}$$

Where $\boldsymbol{m_{TPA,sample}}$ is the mass of crude TPA initially weighed to prepare the sample and $\boldsymbol{m_{TPA,\,calc}}$ is the calculated mass of TPA content in the crude precipitate. Thus, the TPA purity is a weight percentage. TPA peak purity was also determined and compared to TPA mass purity. TPA peak purity was determined according to Eq. 5:

View Article Online
DOI: 10.1039/D5GC02409A

$$TPA\ peak\ purity\ (\%) = \frac{TPA\ peak\ area\ (mAU)}{Total\ peak\ area\ (mAU)} \times 100 \qquad \text{(Eq. 5)}$$

Where $\boldsymbol{Total\ peak\ area\ (mAU)}$ is the sum of all peak areas, excluding internal standard, TMB (t_R = 4.7 min). An exemplary calibration graph, chromatograms and more details on TPA purity determination can be found in the ESI (Figure S13 – S21). Following determination of the crude TPA mass purity (wt%), the pure TPA yield could be determined using Eq. 6:

$$Pure\ TPA\ yield\ (wt\%) = \frac{(m_{TPA}/M_{TPA}) \times TPA\ purity}{m_{PET,\,0}/M_{PET}} \times 100 \qquad \text{(Eq. 6)}$$

Whereby the TPA purity used in the equation is specifically the TPA mass purity determined in accordance with Eq. 4.

Monomer solubility screening

0.1 g TPA mixed with 2.0 g IL solution or solvent (water, acetic acid, 1-methylimidazole, or 1,5-diazabicyclo[4.3.0]non-5-ene) containing 15 wt% water was placed in a 15 mL pressure tube with a Teflon cap and silicon or FETFE O-ring. The tube was heated at 180 °C for 3 h in a pre-heated oven. The solutions were visually inspected while still in the oven to see if the TPA was solubilised and once they had cooled down, a photograph was taken (in Figure S22) and the qualitative observation was recorded.

Results and Discussion

Ionic liquid selection and synthesis of protic ILs

Two imidazolium cations were selected, the aprotic 1,3-dialkylimidazolium cation type and the protic 1-methylimidazolium cation type (Figure 2). ILs with an imidazolium cation are well studied in the literature and relatively stable when heated.[36, 39, 40] Due to the low pK_a of 1-methylimidazole (pK_a = 7.1),[41] an amidinium cation, 1,5-diazabicyclo[4.3.0]non-5-enium ([DBNH]$^+$), with higher pK_a (pK_a = 12.8) [42] was also studied. The higher pK_a of the amidine nitrogen promotes preparation of PILs with a higher degree of proton transfer.[43] An unprecedented variety of anions were chosen which covers a wide range of hydrogen bond acceptor strengths.[39] In addition, an anion with Brønsted acidity ([HSO_4]$^-$) and one with potential to generate Lewis acidic species ([$ZnCl_3$]$^-$) were included. The cation and anion selection was limited to ILs that are water miscible.

PET hydrolysis in ionic liquid-water mixtures

Protocol development with [C_2C_1im][OAc]

The AIL [C_2C_1im][OAc] was used to develop a screening protocol, because high catalytic activity has been reported for PET glycolysis using this IL.[35] After surveying reaction conditions used in

View Article Online
DOI: 10.1039/D5GC02409A

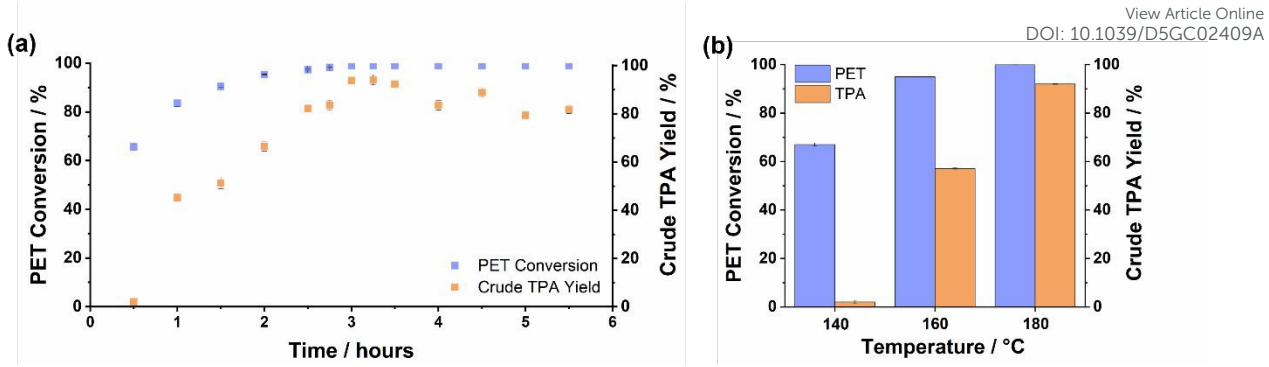

Figure 3: PET hydrolysis in the benchmark IL, $[C_2C_1im][OAc]$ with 15 wt% water. (a) Conversion and isolated crude yield at 180 °C. (b) Impact of reaction temperature on PET conversion and isolated crude TPA yield at 3 h reaction time.

previously published studies on PET depolymerisation, 180°C was chosen as the reaction temperature. PET hydrolysis at lower temperatures has been reported, but requires long reaction times.[44, 45] The requirement for high temperature is assigned to the high crystallinity of PET and the ester bond being stabilised by conjugated benzene ring. The 15 wt% water content represents a balance between retaining the IL as the dominant solvent component by mass, while ensuring that the IL-water mixture is liquid at room temperature and contains an excess of water (16 times more moles of water than PET ester linkages). The 5 wt% PET loading ensured sufficient product for accurate quantification with a microbalance while ensuring complete wetting of plastic particle surface and minimal impact of solid loading on conversion.

PET conversion was observed in the $[C_2C_1im][OAc]$ water mixture (Figure 3) and depolymerisation was confirmed by detecting peaks for TPA and EG in the ^{1}H-NMR spectrum of the post-hydrolysis solution (Figure S23a). The reaction time was varied between 0.5 h and 5.5 h at the screening temperature (Figure 3a), showing that PET conversion reached 100% at around 2.5 h for the $[C_2C_1im][OAc]$ water mixture. The reaction temperature was also varied between 140 and 180 °C, with PET conversion decreasing with lower reaction temperature as expected (Figure 3b). The screening experiments confirmed that an appropriate temperature for 3 h reaction time was 180 °C.

Isolating the crude TPA product

To demonstrate the potential for isolating TPA from the reaction mixtures and focus on the screening, aqueous HCl was added, with pH 3 inducing precipitation. The filtration of the suspension was accompanied by washing with deionised water to afford a white or off-white precipitate, regardless of the IL-water mixture colour post-hydrolysis (Figure S24). ^{1}H-NMR spectroscopic analysis confirmed that the isolated product was mostly TPA (Figure 4). A detailed discussion of the crude TPA composition is presented below.

View Article Online
DOI: 10.1039/D5GC02409A

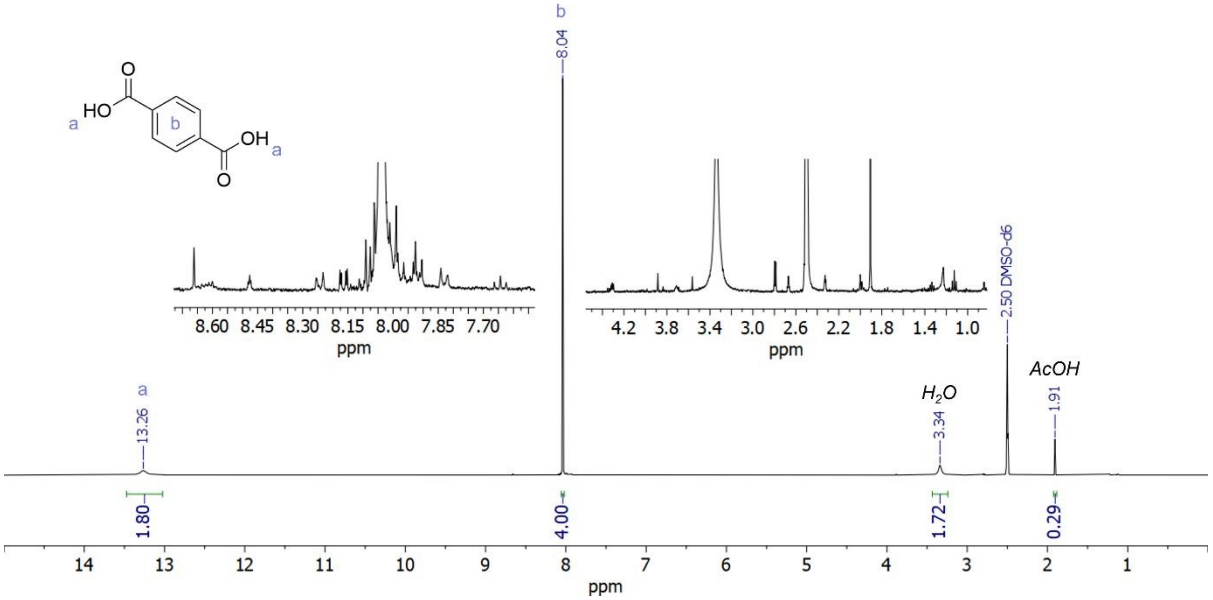

Figure 4: ^{1}H NMR spectrum of the isolated TPA product after PET depolymerisation with [C_2C_1im][OAc] containing 15 wt% water, showing that the product was mainly terephthalic acid. Insets show additional peaks in the aromatic (7.5-8.8 ppm) and aliphatic (1-4.5 pm) regions of the spectrum. Reaction conditions: 3 h, 180 °C, 5 wt% PET loading. NMR solvent: DMSO-d_6.

Interestingly, a lag was observed for PET conversion and TPA yield, the difference being more prominent at shorter reaction times and lower reaction temperatures (Figure 3). A maximum crude TPA yield (92%) was observed at around 3.3 h, which occurred ~50 min after achieving full PET conversion. The lag between PET conversion and crude TPA yield suggests that intermediate depolymerisation products form which are soluble in dilute aqueous acid, potentially glycol terminated oligomers and BHET. A gradual drop in yield at longer times suggests that slower reactions may have affected the purity of the crude product, however, the product purity was not determined for this set of experiments.

View Article Online
DOI: 10.1039/D5GC02409A

Table 1: PET conversion after hydrolysis at 180°C for 3 h in ionic liquid and solvent water mixtures (15 wt%), while the TPA yield was determined gravimetrically following acidification and filtration.

Solvent name	Abbreviation	PET conversion (%)	Isolated crude TPA yield (wt%)
1-Ethyl-3-methylimidazolium acetate	$[C_2C_1im][OAc]$	100.0 ± 0.0	91.9 ± 1.2
1-Butyl-3-methylimidazolium methyl sulfate	$[C_4C_1im][MeSO_4]$	25.9 ± 1.0	0
1-Butyl-3-methylimidazolium methanesulfonate	$[C_4C_1im][MeSO_3]$	32.1 ± 1.2	2.6 ± 0.1
1-Ethyl-3-methylimidazolium hydrogen sulfate	$[C_2C_1im][HSO_4]$	11.2 ± 0.3	0.1 ± 0.0
1-Butyl-3-methylimidazolium hydrogen sulfate	$[C_4C_1im][HSO_4]$	6.7 ± 0.4	0.3 ± 0.1
1-Butyl-3-methylimidazolium chloride	$[C_4C_1im]Cl$	0.1 ± 0.0	0
1-Methylimidazolium acetate	$[C_1Him][OAc]$	98.5 ± 0.4	82.4 ± 2.2
1-Methylimidazolium acetate	$[C_1Him][OAc]$ (1:2)	98.4 ± 0.4	66.5 ± 0.1
1-Methylimidazolium acetate	$[C_1Him][OAc]$ (2:1)	97.5 ± 0.3	59.0 ± 0.3
1-Methylimidazolium chlorozincate	$[C_1Him][ZnCl_3]$	23.0 ± 0.4	0.1 ± 0.0
1-Methylimidazolium triflate	$[C_1Him][OTf]$	9.0 ± 1.2	2.8 ± 0.3
1-Methylimidazolium chloride	$[C_1Him]Cl$	4.9 ± 0.3	0
1-Methylimidazolium hydrogen sulfate	$[C_1Him][HSO_4]$	3.5 ± 0.3	0
1-Methylimidazolium methanesulfonate	$[C_1Him][MeSO_3]$	1.0 ± 0.3	1.5 ± 0.2
Diazabicyclo(4.3.0)non-5-enium acetate	[DBNH][OAc]	100.0 ± 0.0	46.8 ± 0.4
Diazabicyclo(4.3.0)non-5-enium acetate	[DBNH][OAc] (1:2)	100.0 ± 0.0	7.1 ± 0.2
Diazabicyclo(4.3.0)non-5-enium acetate	[DBNH][OAc] (2:1)	98.4 ± 0.0	9.2 ± 0.2
Diazabicyclo(4.3.0)non-5-enium methanesulfonate	$[DBNH][MeSO_3]$	16.1 ± 1.0	0.2 ± 0.1
Diazabicyclo(4.3.0)non-5-enium hydrogen sulfate	$[DBNH][HSO_4]$	12.3 ± 0.1	0.1 ± 0.0
Diazabicyclo(4.3.0)non-5-enium chloride	[DBNH]Cl	11.6 ± 1.1	0
1-Methylimidazole		98.4 ± 0.6	92.5 ± 3.5
Diazabicyclo(4.3.0)non-5-ene		100.0 ± 0.0	16.3 ± 4.4
Acetic acid		62 ± 13	52 ± 12
Water (deionised)		0	0

Effect of solvent composition on hydrolytic PET conversion and TPA yield

Next, the group of selected ILs were employed using the screening condition (180°C, 3 h, 5% PET loading, 15 wt% water). A step was added that employed 1 M aqueous sodium hydroxide before filtration to ensure that all TPA was solubilised as sodium terephthalate, in case a solvent may exhibit good conversion but low solubility for the monomer. Control experiments confirmed that raising the pH to 10 – 11 with 1 M sodium hydroxide did not cause measurable PET hydrolysis during the recovery. The unhydrolysed PET was separated by filtration and dried to determine PET conversion.

PET hydrolysis in acetate ILs

A strong dependency of PET conversion on the nature of the IL anion was observed (Table 1). All acetate ILs showed near-quantitative or quantitative conversion regardless of cation, while the other IL-water mixtures converted 32% PET or less, demonstrating a step change in performance. Despite the high conversion observed in all acetate ILs, the isolated crude TPA yield varied substantially. The reference AIL, $[C_2C_1im][OAc]$, generated the highest crude TPA yield (92%) during the screening, followed by $[C_1Him][OAc]$ (82%) and [DBNH][OAc] (47%) (Figure 5). The monomers TPA and EG in acetate ILs were observed in ^{1}H-NMR spectra

View Article Online
DOI: 10.1039/D5GC02409A

of the post-hydrolysis solution via a singlet peak at 3.4 ppm (EG) and one at 7.8 – 8.0 ppm (TPA) (Figure S23). The study focused on the isolation and purity of larger of the two monomers (TPA) as an indicator of performance, however, attention must be paid to both TPA and EG to develop a viable recycling process.

Conversion and crude TPA yield were also determined for the amines used to generate the protic acetate ILs, for acetic acid (each also containing 15 wt% water) and for deionised water as a control. PET conversion was observed for the three aqueous mixtures in the order DBN > 1-methylimidazole > acetic acid but not in deionised water, demonstrating the need for using an acidic or nucleophilic catalyst. Successful conversion of PET with 1-methylimidazole and diazabicyclo(4.3.0)non-5-ene (DBN) shows that the unprotonated base could play a role in promoting PET depolymerisation,[41, 42] as 1-methylimidazole is a known catalyst for ester hydrolysis and transesterifications via formation of an activated intermediate.[46, 47]

PET hydrolysis in components of protic acetate ILs

A high crude yield upon acidification was obtained for 1-methylimidazole (93%), similar to the yield obtained with [C_2C_1im][OAc] (92%), while the crude TPA yield for DBN was low (16%), mirroring the low yield obtained for [DBNH][OAc]. The low yield could be due to hydrolytic decomposition of both DBN and [DBNH][OAc] at 180 °C, as suggested by the ^{1}H-NMR spectrum of [DBNH][OAc] after heating under the reaction conditions (Figure S25, Table S2).[48, 49] The hydrolytic decomposition of DBN and [DBNH][OAc] uses up water, potentially reducing the amount water available for hydrolysis, while the decomposition product, 3-(aminopropyl)-2-pyrrolidone, contains a primary amine with can react with TPA or acetic acid to form amide bonds (Figure S26).

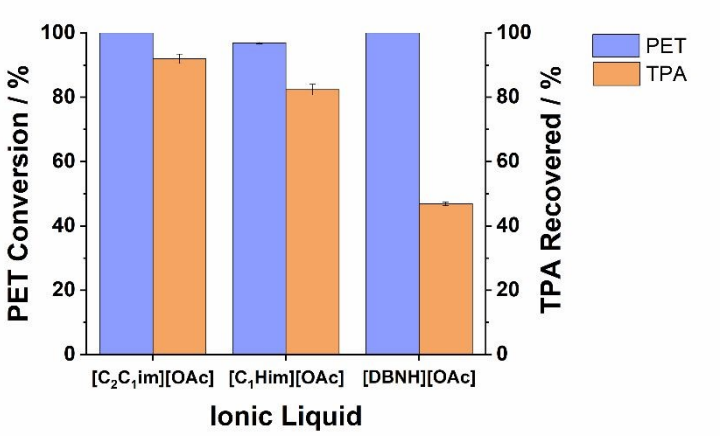

Figure 5: Conversion and recovered crude TPA yield obtained with various acetate ionic liquids. PET was hydrolysed at 180°C for 3 h in the presence of 15 wt% water, with a PET loading of 5%.

Acetic acid generated a lower and more variable PET conversion (~62±13%), with a similar crude TPA yield (~52±12%). It is unclear why the standard errors for the measurements

View Article Online
DOI: 10.1039/D5GC02409A

in acetic acid were large. A control experiment weighing the samples showed that solvent losses were not responsible for the variation in yield.

PET hydrolysis in non-acetate ILs

PET conversion was low in the non-acetate ILs, including the ones containing the chloride anion (0.1 – 11%), which was surprising, as $[C_4C_1im]Cl$ had been reported previously as an effective hydrolysis solvent by Liu *et al*.[36] We repeated the experiment with $[C_4C_1im]Cl$ multiple times, including with the addition of HCl in various amounts based on the hypothesis that the IL used in the previous study may have contained acid impurities, but were unable to reproduce the literature results. The PET conversion could instead perhaps be due to residual alkylimidazole left over from IL synthesis.

Low PET conversion was also observed for the methanesulfonate, methyl sulfate, hydrogen sulfate, triflate and chlorozincate ILs. It has been reported that 1-butyl-3-methylimidazolium chlorozincate, $[C_4C_1im][ZnCl_3]$, and 1-allyl-3-methylimidazolium chlorozincate, $[AllC_1im][ZnCl_3]$, catalyse the transesterification of PET with EG with high conversions (98% and 100%, respectively) and yield BHET as the major product. [50, 51] The results for the PET hydrolysis with a chlorozincate IL demonstrates that ILs effective in catalysing PET glycolysis do not necessarily work for PET hydrolysis.

Effect of acid-to-base ratio in acetate PILs

Since PILs are made by combining an acid and an amine through simple mixing, it is easy to vary the ratio of both components, which can be expressed as the molar acid-to-base ratio (ABR). The ABR is particularly interesting for PILs formed with acetic acid, which are known for incomplete proton transfer from the acid to the base. $[C_1Him][OAc]$ is described as a pseudo-protic IL, whose degree of proton transfer appears to be favoured under excess acid conditions (in the presence of <0.1 wt% water).[52, 53] Hence, molar ABRs other than 1:1 were explored for PET hydrolysis with $[C_1Him][OAc]$ and [DBNH][OAc], one with a 50 mol% excess amine and one with 50 mol% excess acetic acid, while all other reaction parameters remained the same. Figure 6 shows that PET conversion was high for all investigated ABRs, while the crude TPA yield was the highest for the 1:1 ABR for both ILs, demonstrating the importance of ABR as an additional reaction and process parameter for protic ILs.

View Article Online
DOI: 10.1039/D5GC02409A

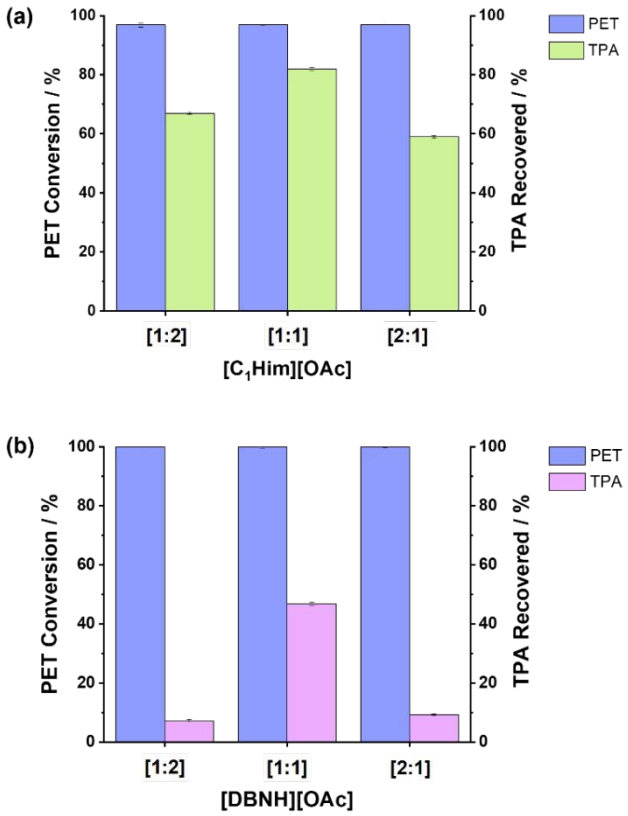

Figure 6: Effect of changing the molar ABR of the protic acetate ILs . (a) [C_1Him][OAc] and (b) [DBNH][OAc] on PET conversion and crude TPA yield.

It is currently unclear how the equimolar stoichiometry achieved the best crude product yield for the protic ILs, however, the solvent composition likely affects the hydrogen bonding network and proton transfer equilibrium, which has been documented for [C_1Him][OAc],[54] and would influence the catalysis in the solvent. Variation of the ABR should be investigated more thoroughly going forward.

Characterisation of crude TPA recovered from acetate ILs and PIL precursors

^{1}H-NMR spectra of the crude precipitates (e.g. Figure 4 and Figure S27) show that the majority of the isolated precipitate was TPA, identified by a singlet peak at 8.0 ppm. The ^{1}H-NMR spectra (Figure 4 and Figure S28) also indicate the presence of other compounds with aromatic (7.2 – 9.0 ppm) and aliphatic signals (0.1 – 5.0 ppm). These are likely depolymerisation products where TPA is esterified with EG (such as the dimer and trimers), while in the case of imidazolium ILs, some of these peaks may be due to the cation. Commercial TPA (Figure S29) also contained impurities that gave ^{1}H-NMR signals (7.8 and 8.2 ppm), which could be the ortho- and meta-dicarboxylic acids. Acetic acid (1.9 ppm) was also found in the precipitates

View Article Online
DOI: 10.1039/D5GC02409A

generated with acetate ILs and with acetic acid. The amount of acetic acid present in the crude product varied between 0.2 and 3.2 wt% of the crude TPA (Table S3).

While ^{1}H-NMR spectroscopy can be used to detect and quantify TPA, EG, and acetic acid, HPLC is a more precise technique for quantification, as it separates TPA from other similar products. Hence, this study implemented a HPLC protocol to analyse selected samples, with the method development discussed in the SI, and data on sample purity shown in Figure 7 and Table S3.

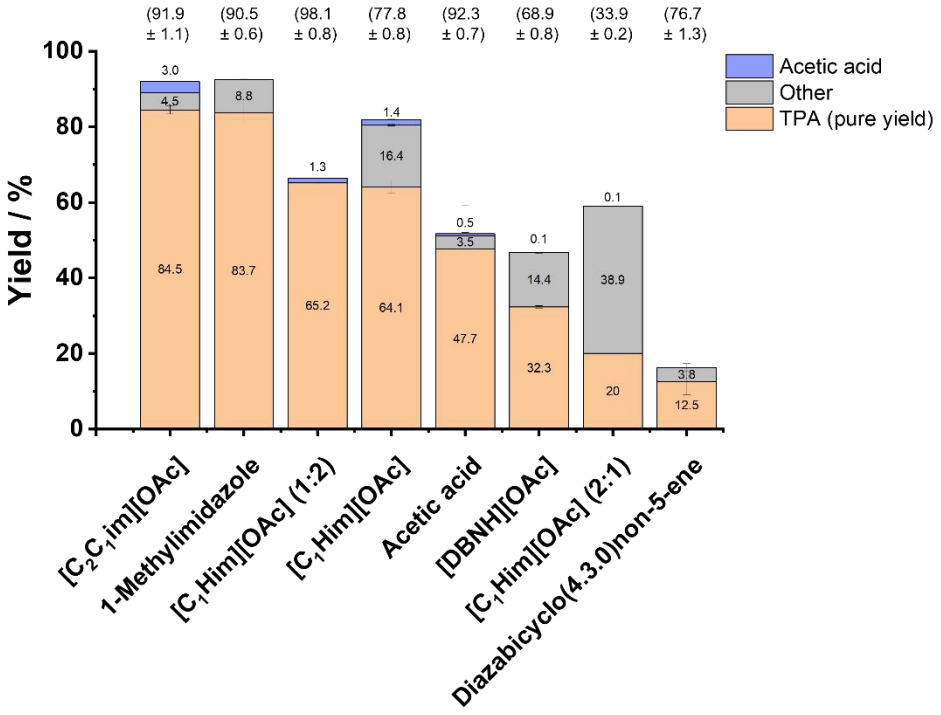

Figure 7 Pure yield of terephthalic acid, adjusted from recovered crude yield and purity (wt%) determined via HPLC. Acetic acid content calculated via ^{1}H-NMR spectroscopy. TPA purity in (wt%) determined by HPLC in brackets above.

This study shows that relying on the crude TPA yield to determine performance is insufficient, and product purity must be considered to draw sound conclusions. The purest TPA product (98 wt%) was obtained with [C_1Him][OAc] with 1:2 ABR, followed by the benchmark IL [C_2C_1im][OAc] (92 wt%). Use of acetic acid and 1-methylimidazole also generated high TPA purities (>90%). For the acetate ILs with 1:1 stoichiometry, TPA purity followed the same trend as the crude TPA yield ([C_2C_1im][OAc]>[C_1Him][OAc]>[DBNH][OAc]). To meet the requirements for polymer-grade TPA (>99%),[55] the crude TPA could be purified via crystallisation, as performed in the Amoco process.[56]

The pure TPA yield was determined by combining TPA purity with the crude TPA yield. The highest pure TPA yield was obtained with [C_2C_1im][OAc] (85%) and 1-methylimidazole (84%), while the lowest pure yields were obtained with [DBNH][OAc] and DBN (32% and 13%), which is likely associated with the decomposition of [DBNH][OAc] and DBN (Figure S26). The

View Article Online
DOI: 10.1039/D5GC02409A

decomposition and reactivity of the decomposition product suggest that performance of the DBN-based IL may not be improved meaningfully with further optimisation. Despite the equimolar composition of [C_1Him][OAc] yielding the highest crude TPA yield, the pure TPA yield obtained with the excess acid composition was similar to the 1:1 composition (65% and 64%, respectively), further demonstrating the importance of ABR as a reaction parameter.

The HPLC analysis detected up to 22 additional compounds in the isolated crude TPA (Figure S30). Among them were the partially hydrolysed products BHET and HETA (Figure S31), which were identified by mass spectroscopy. 20 compounds remained unidentified due to the inability to obtain mass spectra with the LC-MS, however, it is likely that they include incompletely hydrolysed PET fragments, such as dimers, trimers and oligomers, which requires further investigation. Comparison of the TPA purities determined by mass with the ones obtained by peak area confirmed that a significant proportion of impurities was not detected when employing HPLC-UV vis analysis (Table S3), which is limited to compounds that are resolved by the eluent and column combination and are UV active. The difference between mass and area purity was particularly high for precipitates generated with [DBNH][OAc] (Δ = -13%), DBN (Δ = -12%) and [C_1Him][OAc] 2:1 (Δ = -18%), which also generated the lowest crude and pure TPA yields. Overall, the 1:1 and the excess acid composition of [C_1Him][OAc] resulted in the highest pure TPA yield for protic ILs using the screening conditions, suggesting that these solvents may be preferable.

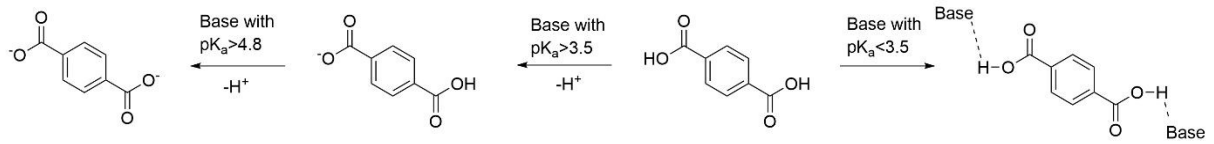

Figure 8: Interaction of terephthalic acid with Brønsted bases of different strengths. Bases that are not strong enough to deprotonate the carboxylic acid groups may coordinate to TPA through hydrogen bonding.

Solubility of TPA in IL-water mixtures

It was hypothesised that effective PET hydrolysis in IL-water mixtures may be linked to high TPA solubility, as removing the product from solid PET into the liquid phase could drive the hydrolysis reaction. Hence, monomer solubility was qualitatively observed at 5 wt% TPA loading for the IL-water mixtures investigated in this study (Table 2). Visual assessments were converted into the categories Yes/No/Partially. TPA solubility was found to be strongly anion dependent. All ILs with the acetate anion completely dissolved 5 wt% TPA at 25°C and 180°C, which is ascribed to the relatively high pK_a of the acetate anion (4.8), leading to deprotonation

of TPA (pK_{a1} 3.5) (Figure 8), including the IL solvents with excess acid and amine. TPA was also highly soluble in the presence of 1-methylimidazole and DBN, which can also be rationalised by the high pK_a of these amines.[41, 42, 57] TPA was not notably soluble in the acetic acid-water mixture and deionised water.

Table 2: Qualitative assessment of the solubility of TPA in the ionic liquid and selected molecular solvents with 15 wt% water. Ionic liquid solutions containing 5 wt% TPA were heated at 180 °C for 3 h.

		Temperature	
		25 °C	180 °C
Methylimidazolium	$[C_1Him][OAc]$	Y	Y
	$[C_1Him][OAc]$ excess AcOH	Y	Y
	$[C_1Him][OAc]$ excess C_1im	Y	Y
	$[C_1Him]Cl$	*Partially*	Y
	$[C_1Him][MeSO_3]$	N	*Partially*
	$[C_1Him][HSO_4]$	N	N
	$[C_1Him][OTf]$	N	N
	$[C_1Him][ZnCl_3]$	N	N
Diazabicyclo(4.3.0)non-5-enium	[DBNH][OAc]	Y	Y
	[DBNH][OAc] excess AcOH	Y	Y
	[DBNH][OAc] excess DBN	Y	Y
	[DBNH]Cl	N	*Partially*
	$[DBNH][MeSO_3]$	Y	Y
	$[DBNH][HSO_4]$	N	N
Dialkylimidazolium	$[C_2C_1im][OAc]$	Y	Y
	$[C_2C_1im][HSO_4]$	N	N
	$[C_4C_1im][OAc]$	Y	Y
	$[C_4C_1im]Cl$	N	*Partially*
	$[C_4C_1im][MeSO_3]$	*Partially*	Y
	$[C_4C_1im][HSO_4]$	N	N
	$[C_4C_1im][MeSO_4]$	N	*Partially*
Molecular Solvents	Acetic acid	N	N
	1-Methylimidazole	Y	Y
	Diazabicyclo(4.3.0)non-5-ene	Y	Y
	De-ionised Water	N	N
	Ethylene glycol	N	N

Full or partial solubilisation of 5 wt% TPA was observed for certain ILs whose anion has a lower pK_a than that of TPA, for example 1-methylimidazolium chloride, $[C_1Him]Cl$, $[C_4C_1im]Cl$ and diazabicyclo(4.3.0)non-5-enium chloride, [DBNH]Cl. This is ascribed to the anion being a strong hydrogen bond acceptor (Kamlet–Taft β parameter = 0.83), as shown in Figure 9. Solubility appeared to be temperature-dependent for these ILs, with better solubility observed at the screening reaction temperature (180 °C).

View Article Online
DOI: 10.1039/D5GC02409A

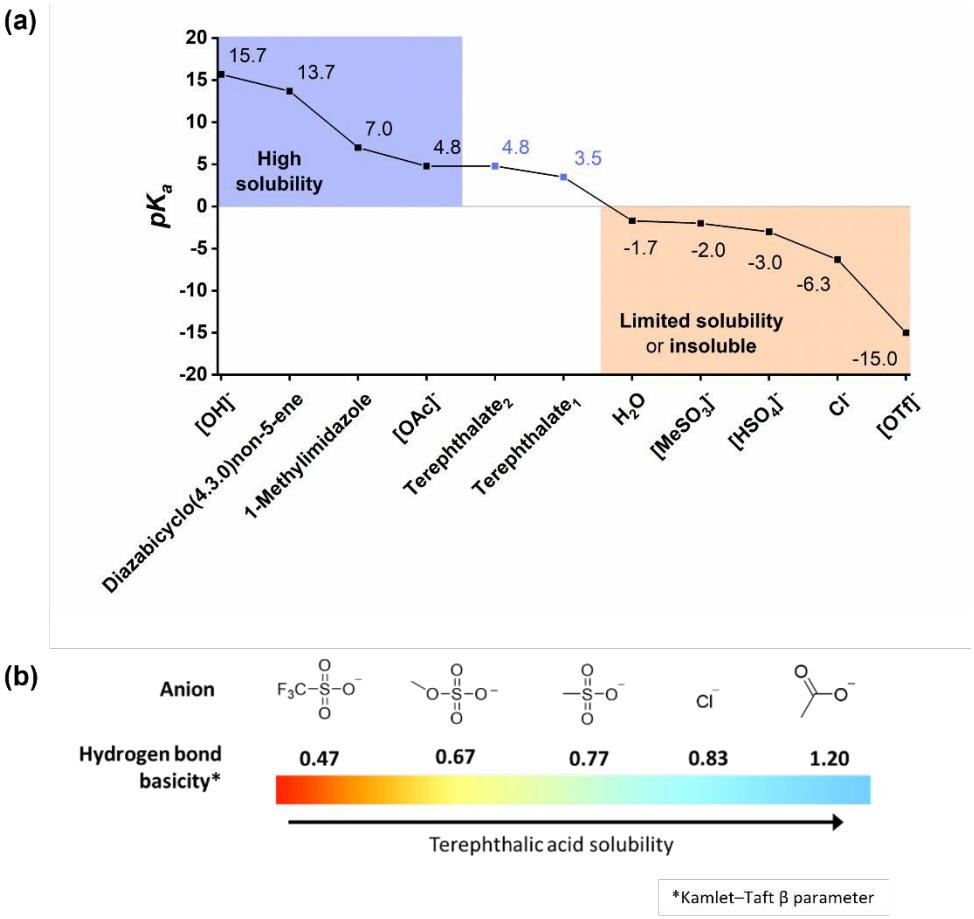

Figure 9: (a) Relationship between pK_a of the corresponding acid of ionic liquid or molecular solvent used in this study and terephthalic acid solubility. Terephthalic acid displays high solubility in Brønsted basic solvents with a high pK_a by generating terephthalate (TPA^{2-}) salts. (b) Relationship between the Kamlet-Taft β parameter of ionic liquids[58] used in this study and terephthalic acid solubility. Solubility in solvents with lower pK_a is nuanced and affected by the ability to form strong hydrogen bonds with TPA, of which the Kamlet-Taft β parameter is an indicator of.

A substantial cation effect was observed for the ILs with chloride and methanesulfonate anions (Figure 10). For methanesulfonate ILs, 5 wt% TPA was insoluble at 25 °C in protic 1-methylimidazolum methanesulfonate, $[C_1Him][MeSO_3]$, completely soluble in aqueous diazabicyclo(4.3.0)non-5-enium methanesulfonate, $[DBNH][MeSO_3]$, and partially soluble in aprotic 1-butyl-3-methylimidazolium methanesulfonate, $[C_4C_1im][MeSO_3]$. It is unclear why the methanesulfonate ILs are subject to a stronger cation effect than the other ILs; the lower pK_a of methanesulfonic acid and the relatively high hydrogen bond basicity (β=0.77) of the methanesulfonate anion may be playing a role.

View Article Online
DOI: 10.1039/D5GC02409A

(a)

25 °C	$[OAc]^-$	Cl^-	$[MeSO_3]^-$	$[HSO_4]^-$	$[OTf]^-$
$[C_1Him]^+$	Y	P	N	N	N
$[DBNH]^+$	Y	N	Y	N	
$[C_nC_1im]^+$	Y	N	P	N	

(b)

180 °C	$[OAc]^-$	Cl^-	$[MeSO_3]^-$	$[HSO_4]^-$	$[OTf]^-$
$[C_1Him]^+$	Y	Y	P	N	N
$[DBNH]^+$	Y	P	Y	N	
$[C_nC_1im]^+$	Y	P	Y	N	

Figure 10: Solubility of TPA in ionic liquids with 15% water shown as a matrix at (a) at 25 °C (b) at 180 °C. ILs ordered according to Kamlet Taft hydrogen bond acceptor strength (high to low from left to right).

5 wt% TPA was not soluble in ILs with a low hydrogen bond acceptor strength, including $[OTf]^-$ and $[ZnCl_3]^-$, nor the ILs with acidic anion and intermediate hydrogen bond basicity, $[C_1Him][HSO_4]$, $[C_4C_1im][HSO_4]$ and diazabicyclo(4.3.0)non-5-enium hydrogen sulfate, $[DBNH][HSO_4]$. This could be due to the acidic anion favouring TPA protonation and hence formation of crystallised TPA. However, 1-butyl-3-methylimidazolium methyl sulfate, $[C_4C_1im][MeSO_4]$, whose anion has a similar Kamlet–Taft β parameter without the acidity, did not promote TPA solubility at 25 °C, while only partial solubility was observed at 180 °C, suggesting that the hydrogen bonding of sulfate anions is generally insufficient. It is possible that transesterification and hydrolysis involving the methyl sulfate anion occur at 180 °C. Some of the qualitative TPA solubilities reported here are in good agreement with quantitative TPA solubilities reported in the literature for water-free ILs.[59] The solubility of TPA in anhydrous ILs was reported as 25 wt%, 10 wt% and 0 wt% for $[C_1Him][OAc]$, $[C_1Him]Cl$ and $[C_1Him][HSO_4]$, respectively.[59]

Figure 11 suggests a correlation between TPA solubility and PET conversion, however, notable exceptions include $[C_1Him]Cl$, $[DBNH][MeSO_3]$ and $[C_4C_1im][MeSO_3]$, which demonstrated substantial TPA solubility yet poor PET conversion (≤26%). At the same time acetic acid provided good PET conversion despite low TPA solubility.

View Article Online
DOI: 10.1039/D5GC02409A

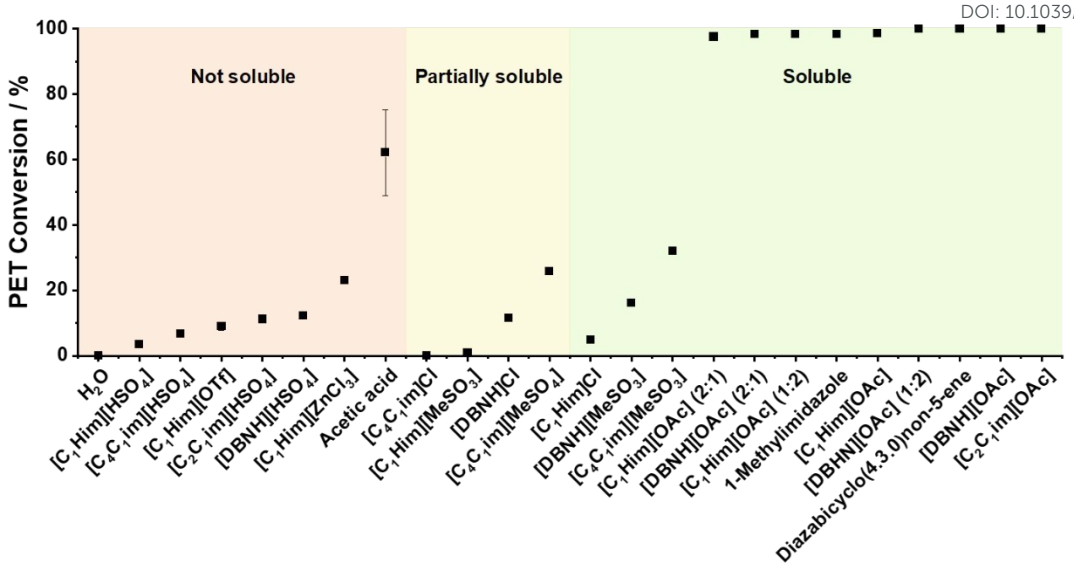

Figure 11: PET conversion in solvent at 180 °C after 3 h with 15 wt% H_2O present ordered according to solubility of 5 wt% TPA at 180 °C in the same solvent mixture.

Overall, it was observed that TPA solubility increased with the hydrogen bonding strength of the IL anion and the pK_a of the anion's corresponding acid (Figure 9). The observations suggest that the anion's hydrogen bond acceptor strength needs to be β>0.67 to achieve good TPA solubility or the pK_a of the corresponding acid of the anion needs to exceed the pK_{a1} of terephthalic acid. Incomplete proton transfer from acid to base for some protic ILs may also enhance TPA solubility, with the unprotonated amine promoting solubility of the dicarboxylic acid through TPA deprotonation.

Consideration of process aspects, including solvent cost and hazards

Solvent recovery and cost are key for developing viable solvent-based chemical processes.[60] IL stability is a concern in PET depolymerisation due to the elevated temperatures required to achieve good PET conversions and TPA yields at an acceptable reaction rate. Solvent and reagent stability provide an upper limit for reaction temperatures. Figure 12 depicts a colour change for the $[C_2C_1im][OAc]$-water mixture, which started as a colourless solution and gradually turned dark brown. The discolouration was accompanied by the appearance of at least four new peaks (δ = 7.6, 7.2, 6.9 and 3.6 ppm) in the ^{1}H-NMR spectrum at ~2 mol% (Figure S32 and Table S4), which suggests dealkylation of 1-ethyl-3-methylimidazolium by acetate to 1-alkylimidazoles and esters of acetic acid. This was expected given the low stability of anhydrous $[C_2C_1im][OAc]$ at 180 °C.[61, 62] Interestingly, this decomposition may not lower performance in this application, given that 1-methylimidazole also promoted PET hydrolysis.

View Article Online
DOI: 10.1039/D5GC02409A

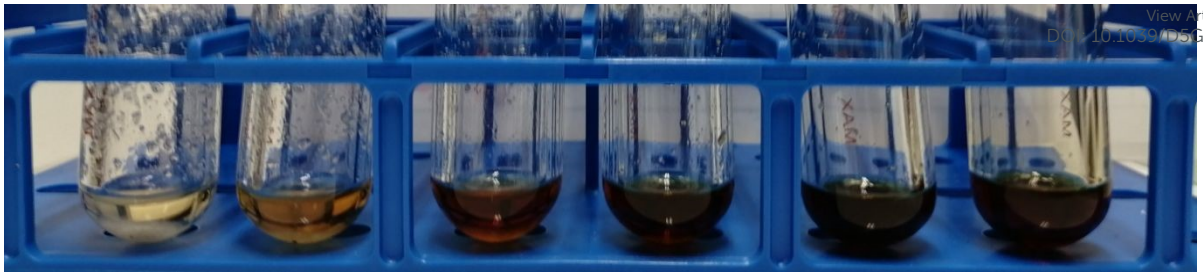

Figure 12: Samples containing [C_2C_1im][OAc] with 15% w/w water and 5 wt% shredded bottle PET heated at 180 °C as a function of time. Hydrolysis duration from 0.5 h (left) to 3 h (right) in 0.5 h increments.

Varying degrees of discolouration were observed for the other ILs after PET depolymerisation (Figure S33), except for [C_4C_1im][$MeSO_3$]. The ^{1}H-NMR spectrum of [DBNH][OAc] after applying the screening condition was examined and revealed the appearance of seven new peaks, suggesting again the presence of the ring-opened hydrolysis product (Figure S25 and Table S2).[49] This decomposition may be linked to the lower performance of the [DBNH][OAc] water mixture, as discussed earlier. In other cases, decomposition products were not observed in the ^{1}H-NMR spectra, despite the solvent becoming strongly coloured during heating, for example, the [C_1Him][OAc] water mixture (Figure S34 and Table S5). A more thorough and quantitative study of the link between PET hydrolysis performance and IL stability under process conditions should be carried out in the future.

[C_1Him][OAc] emerged from this study as a promising candidate, with good performance (PET conversion, TPA yield and purity) and stability. Hence, we estimated the cost of the IL using a process model developed by Chen *et al.*[63] and compared it to the cost of the aprotic [C_2C_1im][OAc] (Table 3), which requires a more complex synthesis involving alkylation of the alkylimidazole and ion exchange. Details of the calculations can be found in the ESI (Table S6). The cost estimate reveals that the production cost for the [C_1Him][OAc]-water mixture is <10% of the cost of [C_2C_1im][OAc], whose synthesis was modelled as an alkylation of methylimidazole with ethyl chloride followed by ion exchange.[64] The model assumes that solvent cost are dominated by input cost for protic ILs at scale.[63] The cost differences are due to synthetic complexity of the route for aprotic versus protic ILs.

In our cost estimate, excess acid in the IL reduced the solvent cost, due to acetic acid being the cheaper component. A higher water content for hydrolysis may also reduce cost further, hence increasing the water content should be investigated further. The estimated cost of the [C_1Him][OAc]-water compositions is in the range of common organic solvents, such as acetone and ethyl acetate (1.30 – 1.40 $/kg).[63]

View Article Online
DOI: 10.1039/D5GC02409A

Table 3: Estimated solvent cost for $[C_2C_1][OAc]$-water and $[C_1Him][OAc]$-water mixtures used in this study. Cost estimate for anhydrous $[C_2C_1im][OAc]$ ($35/kg) adapted from Morales,[64] utility cost for process water from Turtin et al.[65]

Solvent	Cost of amine ($/kg of IL)	Cost of acid ($/kg of IL)	Cost of water ($/kg)	Solvent cost ($/kg of IL water mixture)
$[C_2C_1im][OAc]$+15% water	N/A	N/A		$29.8
$[C_1Him][OAc]$+15% water	$1.84	$0.27	1.77×10^{-4}	$2.11
$[C_1Him][OAc]$ (1:2)+15% water	$1.29	$0.38		$1.67

When designing a sustainable chemical process, solvent hazards should also be considered, although use of a hazardous solvent can result in an overall more sustainable chemical process.[66] ILs are currently produced at a small scale and hence limited commercial toxicity data are available. For example, the $[OTf]^-$ anion is undesirable, as it is fluorinated and hence likely persistent in the environment, while the Zn-containing anion is undesirable as Zn is a toxic heavy metal. 1-Methylimidazole has moderate toxicity, however, it has recently been classified as a teratogen under European REACH legislation. DBN is imported in the EU <1 tonne and hence does not have a REACH dossier. It is noted for its corrosiveness which is typical for amines. Acetic acid is also corrosive in concentrated form and is classed as a flammable liquid but has otherwise low toxicity and is readily biobased. Decomposition products may modulate the solvent toxicity profile. The chemical hazards of the solvent need to be balanced with the benefit of a potential chemical recycling process and compared to the hazards and environmental impact of TPA and EG production from new (fossil) feedstocks.

The addition of an acid to precipitate the TPA from solution as carried out here changes the composition of the IL,[23, 57] making chemical PET recycling as carried out in this screening study uneconomical while increasing environmental burdens by requiring fresh solvent. Recovery of TPA by antisolvent crystallisation (with water) and EG by distillation would be preferable and will be investigated for the lead solvent going forward.

PET depolymerisation mechanism in IL water mixtures

Using the data collected in this study, general features of the depolymerisation mechanism in IL water mixtures can be discussed. The rate of organic reactions is determined by electronic and steric factors and mass transport. Since PET is insoluble in the IL water mixtures, PET hydrolysis requires the cleavage of ester linkages at the solid-liquid interface. Formation of cracks confirms that depolymerisation occurs at the surface of PET particles,[16, 51, 67] and the shrinking-core kinetic model is often assumed.[17, 18] Reactions at the solid liquid interface are often slowed down due to mass transfer limitations, especially if the viscosity is high, however,

View Article Online
DOI: 10.1039/D5GC02409A

differences in viscosity do not seem to explain the large variation in the observed PET conversion and TPA yield.

Ester hydrolysis is known to proceed via a tetrahedral intermediate (Figure 13),[68] and its formation can be catalysed by acid or base. It is proposed that the reactive IL solvents enable a base catalysed mechanism, as the anion (acetate) can deprotonate water via an equilibrium, generating hydroxide ions which are strong nucleophiles. Hydroxide ions can also be generated via an equilibrium involving water and the amines, which could explain why 1-methylimidazole and DBN water mixtures achieved high PET conversion. In addition, deprotonation of TPA drives conversion by shifting the equilibrium to the product side, which may also play a role why PET conversion is high compared to other ILs.

View Article Online
DOI: 10.1039/D5GC02409A

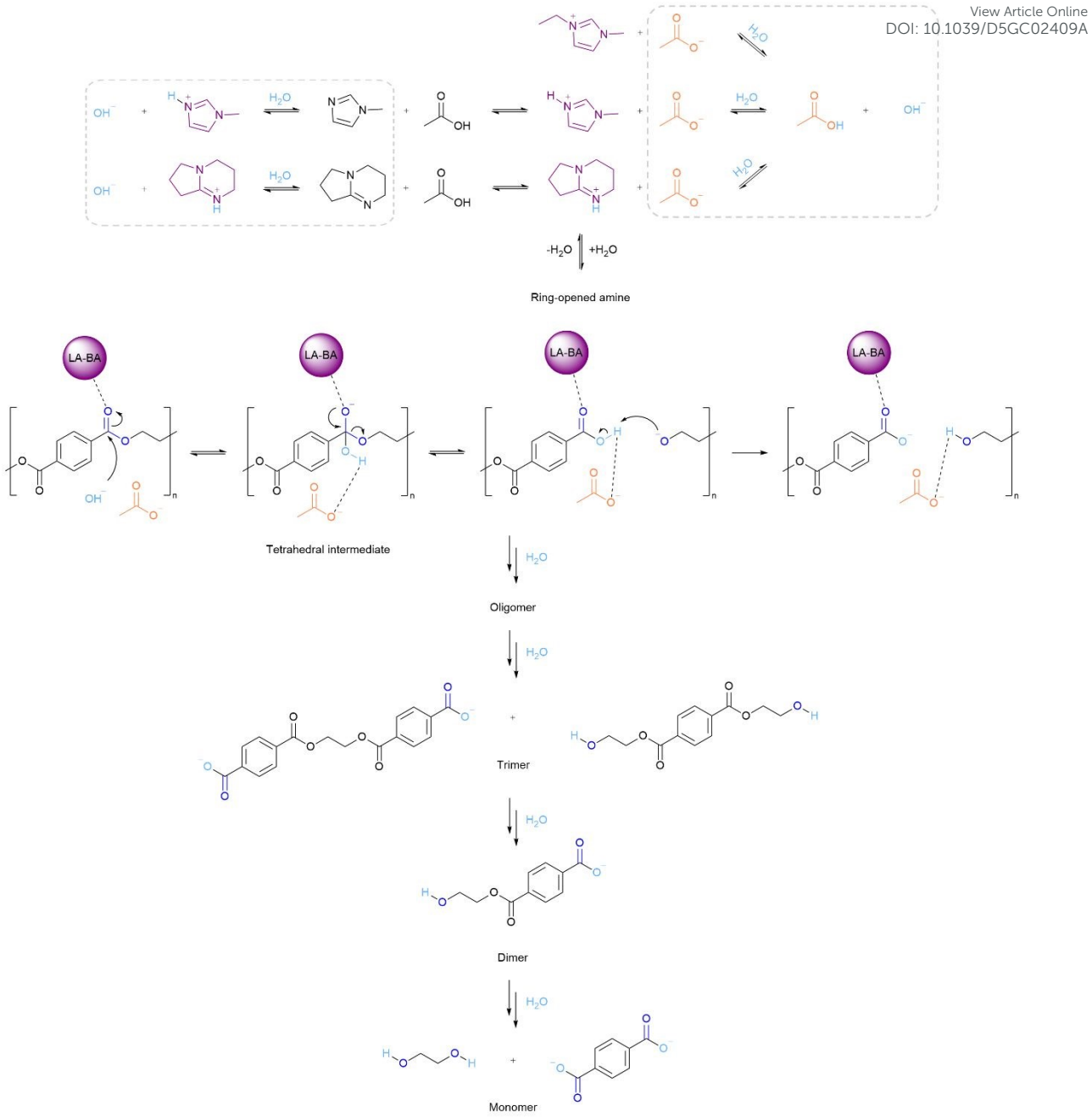

Figure 13: Proposed IL-catalysed PET hydrolysis reaction mechanism using Aprotic and Protic acetate ILs.

It is proposed that of the two protic acetate ILs, only [HC_1im][OAc] ILs supplies noticeable quantities of amine,[54] due to the relatively low pK_a difference between amine and acetic acid (ΔpK_a <3). The high PET conversion for acetate ILs, methylimidazole and DBN can be explained by the (irreversible) deprotonation of TPA and carboxylic acid end groups of short oligomers, hence their reactivity is well-correlated with solubility. The data show that all tested ILs reduce the activation energy compared to water, which is a weak nucleophile. However, they require higher temperatures (at the same reaction time) compared to aqueous solutions of NaOH, due to the lower OH^- concentration.

View Article Online
DOI: 10.1039/D5GC02409A

The cation has been assigned a stabilising role for the tetrahedral intermediate,[18, 38, 69, 70] however, our data do not provide evidence for specific interactions, especially since a number of Brønsted acidic sites are present, such as on the cation, hydronium ions and acetic acid. Generally, activation of the carbonyl group is more important for the acid catalysed ester hydrolysis mechanism than for the base catalysed mechanism. In support of the proposed mechanism, proton affinity (correlated to the Kamlet Taft parameter β) of ILs was reported to determine the reaction rate for esterification (the reverse reaction of hydrolysis).[71] It is proposed that in acetic acid water mixtures, the acid catalysed ester hydrolysis mechanism is applicable. These mechanistic considerations are suggestions and require deeper investigation.

Conclusions

This screening study found that hydrolysis of shredded bottle PET in IL-water mixtures strongly depends on anion selection. PET hydrolysis with the aprotic IL [C_2C_1im][OAc] yielded a screening condition (180 °C, 3 h, 15 wt% H_2O, 5% PET loading), which was successfully used to evaluate a library of aprotic and protic ILs. ILs with acetate anions gave the highest PET conversion and the highest isolated TPA yields (after dilution and acidification), regardless of whether they were protic or aprotic ILs. It was also found that measuring the percentage yield of precipitated product typically overestimates TPA yield, as other hydrolysis products and solvent impurities are present in the crystallised product, shown by ^{1}H-NMR spectroscopy and HPLC.

The pseudo-protic IL [C_1Him][OAc] performed well in the screening, enabling high PET conversion (99%) and crude TPA yield (82 %), and good TPA content (78%) in the isolated crude TPA at acceptable temperatures, with 10 times lower solvent cost than the aprotic [C_2C_1im][OAc], which is encouraging for further study and process development. The IL-water mixtures based on [C_1Him][OAc] at 1:1 and 1:2 ABR generated similar TPA yields, showing that increasing the ABR can be used to lower solvent cost.

Solubility of TPA could be correlated with the strength of interactions between the carboxylic acid groups in TPA and the anion of the IL, as found for other solutes containing hydroxyl groups such as cellulose or lignin.[39] The pK_a of the IL anion exceeding the pK_a of terephthalate was a strong predictor of TPA solubility. Strong hydrogen bond acceptance could also promote solubilisation of TPA, even if the pK_a of the anion was below the threshold. TPA solubility was generally correlated with PET conversion, but some IL solvents with notable TPA solubility displayed low PET conversion at the screening condition. Based on the available data, it is proposed that acetate ILs promote depolymerisation of PET via the base catalysed ester

View Article Online
DOI: 10.1039/D5GC02409A

hydrolysis mechanism, driven by TPA deprotonation. Based on the promising results observed for [C_1Him][OAc]-water mixtures, a waste-free recovery method for the monomers TPA and EG should be developed, which is underway in our laboratory.

Conflicts of interest

The authors have no conflicts to declare.

Acknowledgements

We acknowledge funding of the work via EP/S025456/1, NE/W503198/1, EP/R513052/1 and EP/S023232/1. The authors thank Ruhi Patel and Reeya Patel for assistance in preliminary experiments, Tom Welton for advice, and Chris Roberts from the Centre for Rapid Online Analysis of Reactions (ROAR) facility for assisting with the development of the HPLC method, funded via EP/R008825/1 and EP/V029037/1.

Credit statement (using CRediT)

MYS contributed investigation, writing - original draft, formal analysis and visualisation. HLJ contributed methodology, investigation, formal data analysis and visualisation. PB contributed methodology and investigation. PF contributed conceptualisation, funding acquisition and supervision. JPH contributed conceptualisation, funding acquisition and supervision. ABT contributed conceptualisation, funding acquisition, supervision and project administration. All authors contributed to writing - reviewing and editing.

Notes and references

1. R. Geyer, J. R. Jambeck and K. L. Law, *Sci Adv*, 2017, **3**, e1700782.
2. A. Rahimi and J. M. García, *Nature Reviews Chemistry*, 2017, **1**, 0046.
3. K. Kaiser, M. Schmid and M. Schlummer, *Recycling*, 2017, **3**.
4. *Plastics - the Facts 2022*, Plastics Europe, 2022.
5. D. K. Schneiderman and M. A. Hillmyer, *Macromolecules*, 2017, **50**, 3733-3749.
6. G. P. Karayannidis and D. S. Achilias, *Macromol. Mater. Eng.*, 2007, **292**, 128-146.
7. A. C. Castillo, M. Malakkal, P. Bexis and K. Brophy, *Enabling a greener plastic future through molecular science*, Imprerial College London, Institute for Molecular Sciences and Engineering, 2020.
8. M. Babaei, M. Jalilian and K. Shahbaz, *Journal of Environmental Chemical Engineering*, 2024, **12**, 112507.
9. G. W. Coates and Y. D. Y. L. Getzler, *Nature Reviews Materials*, 2020, DOI: 10.1038/s41578-020-0190-4.
10. Y.-H. V. Soong, M. J. Sobkowicz and D. Xie, *Bioengineering*, 2022, **9**, 98.
11. K. Ragaert, L. Delva and K. Van Geem, *Waste management (New York, N.Y.)*, 2017, **69**, 24-58.
12. B. Geyer, G. Lorenz and A. Kandelbauer, *eXPRESS polymer letters*, 2016, **10**, 559-586.

13. Y. Peng, J. Yang, C. Deng, J. Deng, L. Shen and Y. Fu, *Nature Communications*, 2023, **14**, 3249.
14. T. Uekert, J. S. DesVeaux, A. Singh, S. R. Nicholson, P. Lamers, T. Ghosh, J. E. McGeehan, A. C. Carpenter and G. T. Beckham, *Green Chemistry*, 2022, **24**, 6531-6543.
15. L. Cottam and R. P. Sheldon, *Nature*, 1965, **205**, 1005-1005.
16. A. M. Al-Sabagh, F. Z. Yehia, A.-M. M. F. Eissa, M. E. Moustafa, G. Eshaq, A.-R. M. Rabie and A. E. ElMetwally, *Industrial & Engineering Chemistry Research*, 2014, **53**, 18443-18451.
17. Y. Liu, X. Yao, H. Yao, Q. Zhou, J. Xin, X. Lu and S. Zhang, *Green Chemistry*, 2020, **22**, 3122-3131.
18. R. Zhang, X. Zheng, X. Yao, K. Song, Q. Zhou, C. Shi, J. Xu, Y. Li, J. Xin, I. E.-T. El Sayed and X. Lu, *Industrial & Engineering Chemistry Research*, 2023, **62**, 11851-11861.
19. G. Grause, J. Sutton, A. P. Dove, N. A. Mitchell and J. Wood, *Crystal Growth & Design*, 2024, **24**, 7306-7321.
20. T. Wang, X. Gong, C. Shen, G. Yu and X. Chen, *Polymer Degradation and Stability*, 2021, **190**, 109601.
21. C. N. Onwucha, C. O. Ehi-Eromosele, S. O. Ajayi, M. Schaefer, S. Indris and H. Ehrenberg, *Industrial & Engineering Chemistry Research*, 2023, **62**, 6378-6385.
22. S. Ügdüler, K. M. Van Geem, R. Denolf, M. Roosen, N. Mys, K. Ragaert and S. De Meester, *Green Chemistry*, 2020, **22**, 5376-5394.
23. M. Rollo, F. Raffi, E. Rossi, M. Tiecco, E. Martinelli and G. Ciancaleoni, *Chemical Engineering Journal*, 2023, **456**, 141092.
24. O. A. Attallah, M. Azeem, E. Nikolaivits, E. Topakas and M. B. Fournet, *Polymers*, 2022, **14**, 109.
25. I. Cano, C. Martin, J. A. Fernandes, R. W. Lodge, J. Dupont, F. A. Casado-Carmona, R. Lucena, S. Cardenas, V. Sans and I. de Pedro, *Applied Catalysis B: Environmental*, 2020, **260**, 118110.
26. A. M. Al-Sabagh, F. Z. Yehia, A. M. F. Eissa, M. E. Moustafa, G. Eshaq, A. M. Rabie and A. E. ElMetwally, *Polymer Degradation and Stability*, 2014, **110**, 364-377.
27. T. Wang, C. Shen, G. Yu and X. Chen, *Polymer Degradation and Stability*, 2022, **203**, 110050.
28. C. Jehanno, I. Flores, A. P. Dove, A. J. Müller, F. Ruipérez and H. Sardon, *Green Chemistry*, 2018, **20**, 1205-1212.
29. R. Zhang, X. Zheng, X. Cheng, J. Xu, Y. Li, Q. Zhou, J. Xin, D. Yan and X. Lu, *Materials*, 2024, **17**, 1583.
30. C. Zhu, L. Yang, C. Chen, G. Zeng and W. Jiang, *Physical Chemistry Chemical Physics*, 2023, **25**, 27936-27941.
31. J. D. Badia, R. Ballesteros-Garrido, A. Gamir-Cobacho, O. Gil-Castell and A. Cháfer, *Journal of Environmental Chemical Engineering*, 2024, **12**, 113134.
32. N. Liu, Y. S. Ma, K. W. Shu, B. Wu and D. Zhang, *Advanced Materials Research*, 2014, **893**, 23-26.
33. R. M. Musale and S. R. Shukla, *The Journal of The Textile Institute*, 2017, **108**, 467-471.
34. C. Dou, H. Choudhary, Z. Wang, N. R. Baral, M. Mohan, R. A. Aguilar, S. Huang, A. Holiday, D. R. Banatao, S. Singh, C. D. Scown, J. D. Keasling, B. A. Simmons and N. Sun, *One Earth*, 2023, **6**, 1576-1590.
35. J. Sun, D. Liu, R. P. Young, A. G. Cruz, N. G. Isern, T. Schuerg, J. R. Cort, B. A. Simmons and S. Singh, *ChemSusChem*, 2018, **11**, 781-792.
36. F. Liu, X. Cui, S. Yu, Z. Li and X. Ge, *Journal of Applied Polymer Science*, 2009, **114**, 3561-3565.
37. A. S. Amarasekara, J. A. Gonzalez and V. C. Nwankwo, *Journal of Ionic Liquids*, 2022, **2**, 100021.

38. Z. Zhao, J. Bai, H. Tao, S. Wang, K. Wang, W. Lin, L. Jiang, H. Li and C. Wang, *Green Chemical Engineering*, 2024, DOI: https://doi.org/10.1016/j.gce.2024.12.001.
39. A. Brandt, J. Grasvik, J. P. Hallett and T. Welton, *Green Chemistry*, 2013, **15**, 550-583.
40. A. J. Greer, J. Jacquemin and C. Hardacre, *Molecules*, 2020, **25**, 5207.
41. D. Sanna, V. Ugone, G. Micera, P. Buglyó, L. Bíró and E. Garribba, *Dalton Transactions*, 2017, **46**, 8950-8967.
42. C. Wiles and P. Watts, *Beilstein Journal of Organic Chemistry*, 2011, **7**, 1360-1371.
43. S. Kaiho, A. A. R. Hmayed, K. R. Delle Chiaie, J. C. Worch and A. P. Dove, *Macromolecules*, 2022, **55**, 10628-10639.
44. L. Cosimbescu, D. R. Merkel, J. Darsell and G. Petrossian, *Industrial & Engineering Chemistry Research*, 2021, **60**, 12792-12797.
45. G. P. Karayannidis, A. P. Chatziavgoustis and D. S. Achilias, *Advances in Polymer Technology*, 2002, **21**, 250-259.
46. G. O. Andrés, A. M. Granados and R. H. de Rossi, *The Journal of Organic Chemistry*, 2001, **66**, 7653-7657.
47. P. A. R. Pires, N. I. Malek, T. C. Teixeira, T. A. Bioni, H. Nawaz and O. A. E. Seoud, *Industrial Crops and Products*, 2015, **77**, 180-189.
48. F. S. Pereira, D. Lincon da Silva Agostini, R. D. do Espírito Santo, E. R. deAzevedo, T. J. Bonagamba, A. E. Job and E. R. P. González, *Green Chemistry*, 2011, **13**, 2146-2153.
49. A. Parviainen, R. Wahlström, U. Liimatainen, T. Liitiä, S. Rovio, J. K. J. Helminen, U. Hyväkkö, A. W. T. King, A. Suurnäkki and I. Kilpeläinen, *RSC Advances*, 2015, **5**, 69728-69737.
50. Q. F. Yue, H. G. Yang, M. L. Zhang and X. F. Bai, *Advances in Materials Science and Engineering*, 2014, **2014**, 454756.
51. Q. Wang, X. Lu, X. Zhou, M. Zhu, H. He and X. Zhang, *Journal of Applied Polymer Science*, 2013, **129**, 3574-3581.
52. L. Wylie, M. Kéri, A. Udvardy, O. Hollóczki and B. Kirchner, *ChemSusChem*, 2023, **16**, e202300535.
53. K. Chen, Y. Wang, J. Yao, H. Li and 2018, **122**, 309-315.
54. H. Watanabe, N. Arai, H. Jihae, Y. Kawana and Y. Umebayashi, *Journal of Molecular Liquids*, 2022, **352**, 118705.
55. N. S. Allen, M. Edge, J. Daniels and D. Royall, *Polymer Degradation and Stability*, 1998, **62**, 373-383.
56. R. A. F. Tomás, J. C. M. Bordado, J. F. P. Gomes and R. J. Sheehan, in *Ullmann's Encyclopedia of Industrial Chemistry*, DOI: https://doi.org/10.1002/14356007.a26_193.pub3, pp. 1-17.
57. J. P. Mészáros, W. Kandioller, G. Spengler, A. Prado-Roller, B. K. Keppler and É. A. Enyedy, *Journal*, 2023, **15**.
58. M. A. Ab Rani, A. Brant, L. Crowhurst, A. Dolan, M. Lui, N. H. Hassan, J. P. Hallett, P. A. Hunt, H. Niedermeyer, J. M. Perez-Arlandis, M. Schrems, T. Welton and R. Wilding, *Physical Chemistry Chemical Physics*, 2011, **13**, 16831-16840.
59. K. Matuszek, E. Pankalla, A. Grymel, P. Latos and A. Chrobok, *Molecules*, 2020, **25**, 80.
60. H. Baaqel, I. Díaz, V. Tulus, B. Chachuat, G. Guillén-Gosálbez and J. P. Hallett, *Green Chemistry*, 2020, **22**, 3132-3140.
61. J. D. Oxley, T. Prozorov and K. S. Suslick, *Journal of the American Chemical Society*, 2003, **125**, 11138-11139.
62. M. T. Clough, K. Geyer, P. A. Hunt, J. Mertes and T. Welton, *Physical Chemistry Chemical Physics*, 2013, **15**, 20480-20495.
63. L. Chen, M. Sharifzadeh, N. Mac Dowell, T. Welton, N. Shah and J. P. Hallett, *Green Chemistry*, 2014, **16**, 3098-3106.
64. M. Morales, DOI: 10.3929/ethz-a-010797794, ETH Zurich, 2016.

65. R. Turton, J. A. Shaeiwitz, D. Bhattacharyya and W. B. Whiting, *Analysis, synthesis, and design of chemical processes*, Prentice Hall, Boston, Fifth edition / Richard Turton, Joseph A. Shaeiwitz, Debangsu Bhattacharyya, Wallace B. Whiting. edn., 2018.
66. T. Welton, *Proceedings of the Royal Society A: Mathematical, Physical and Engineering Sciences*, 2015, **471**, 20150502.
67. X. Zhou, X. Lu, Q. Wang, M. Zhu and Z. Li, *Pure and Applied Chemistry*, 2012, **84**, 789-801.
68. J. Clayden, N. Greeves, S. Warren and P. Wothers, *Organic Chemistry*, Oxford University Press, Oxford, 1 edn., 2001.
69. H. Wang, , Z. Li, , Y. Liu, , X. Zhang, , S. Zhang and 2009, **11**, 1568-1575.
70. F. Scé, I. Cano, C. Martin, G. Beobide, Ó. Castillo and I. de Pedro, *New Journal of Chemistry*, 2019, **43**, 3476-3485.
71. T. P. Wells, J. P. Hallett, C. K. Williams and T. Welton, *The Journal of Organic Chemistry*, 2008, **73**, 5585-5588.

View Article Online
DOI: 10.1039/D5GC02409A

Data availability statement

The data supporting this article have been included as part of the Supplementary Information. Data for this article, including electronic forms of the NMR spectra and spreadsheets will be made available at GitHub following peer review at [URL – format https://doi.org/DOI].